Liquid Crystals
Publication details, including instructions for authors and subscription information:
http://www.informaworld.com/smpp/title~content=t713926090

Model-independent structure and resonant X-ray spectra of intermediate smectic phases

Mikhail A. Osipov[a]; Maxim V. Gorkunov[ab]
[a] Department of Mathematics, University of Strathclyde, Glasgow G1 1XH, UK [b] Institute of Crystallography of the Russian Academy of Sciences, Moscow 119333, Russia

To cite this Article Osipov, Mikhail A. and Gorkunov, Maxim V.(2006) 'Model-independent structure and resonant X-ray spectra of intermediate smectic phases', Liquid Crystals, 33: 10, 1133 — 1141
To link to this Article: DOI: 10.1080/02678290601008489
URL: http://dx.doi.org/10.1080/02678290601008489

Liquid Crystals, Vol. 33, No. 10, October 2006, 1133–1141

Model-independent structure and resonant X-ray spectra of intermediate smectic phases

MIKHAIL A. OSIPOV*† and MAXIM V. GORKUNOV†,‡
†Department of Mathematics, University of Strathclyde, 26 Richmond Street, Glasgow G1 1XH, UK
‡Institute of Crystallography of the Russian Academy of Sciences, Leninski pr. 59, Moscow 119333, Russia

(*Received 6 February 2006; in final form 13 June 2006; accepted 1 July 2006*)

It is shown that the orientational structure of intermediate smectic phases can be determined using the symmetry properties of the general free energy with arbitrary orientational coupling between smectic layers, without addressing a particular model. The structure of three- and four-layer intermediate phases, obtained in this way, corresponds to experimental data. The same method enables one to predict the structure of intermediate phases with periodicity of five and six layers, which have not been observed experimentally so far. The resonant X-ray spectra of the five- and six-layer intermediate phases with predicted structure have also been calculated. These spectra are characterized by a number of features which enable one to distinguish five-layer and six-layer intermediate phases from phases with smaller periods.

1. Introduction

Tilted smectic liquid crystals exist in several variants, and the two most important phases are the synclinic SmC phase and the anticlinic $\mathrm{SmC_A}$ phase. In the ideal synclinic phase, both the absolute value and the direction of the director tilt are the same in all layers, while in the anticlinic phase the direction of the tilt alternates from layer to layer. If the tilted smectic phase is chiral, each smectic layer possesses a spontaneous polarization perpendicular to the tilt plane [1, 2]. In the bulk, chiral tilted phases are also characterized by a helical structure with a macroscopic pitch. The exception is the so-called SmC_α^* phase with a short pitch of the order of few smectic periods.

In liquid crystal materials exhibiting both synclinic SmC* and anticlinic $\mathrm{SmC_A^*}$ phases, intermediate smectic phases are often found in the frustration region between the synclinic and anticlinic phases. In some cases, the synclinic SmC* phase is replaced by the SmC_α^* phase as the first phase which is formed directly below the non-tilted SmA* phase. So far intermediate phases have been observed only in chiral liquid crystals, while the syn- and anti-clinic phases themselves are not directly related to molecular chirality. One notes that the synclinic structure is far more common than the anticlinic one. The anticlinic phase has been observed only in selected classes of smectic materials including racemic mixtures [3–5] and a few non-chiral one-component materials [6]. Recently the intermediate phases have attracted significant attention, in particular after their non-trivial structure has been revealed by the resonant X-ray technique [7–10] and ellipsometry [11, 12]. It has been shown that the existing intermediate phases are characterized by the periodicity of three or four smectic layers and possess an unusual three-dimensional chiral stricture. Very recently the variety of liquid crystal materials exhibiting intermediate phases has increased significantly due to the discovery of such phases in binary mixtures of syn- and anti-clinic smectics [13–15]. In such mixtures an intermediate phase may be stable within a temperature interval of about 50°.

In recent years a number of theoretical models have been proposed to explain the origin and structure of the intermediate phases [16–20]. In particular, it has been shown [17] that the experimentally observed 3D structure of the intermediate phases can be derived in the framework of a relatively simple model [16, 21] without additional assumptions based on actual experimental data. It should be noted that several theoretical models, which mainly differ in the nature of the long range interlayer interaction [17, 19, 20] predict the existence of additional intermediate phases with periods larger than four smectic layers, including the phases with five- and six-layer periodicity. Such phases have not been observed so far. It has been shown recently [22] that this may be related to strong long range interlayer interaction of the type proposed by Bruinsma and Prost [23] which has a tendency to suppress intermediate phases with long periods. At the same time, the temperature intervals of

---

*Corresponding author. Email: osipov@maths.strath.ac.uk

Liquid Crystals
ISSN 0267-8292 print/ISSN 1366-5855 online © 2006 Taylor & Francis
http://www.tandf.co.uk/journals
DOI: 10.1080/02678290601008489

the three- and four-layer subphases may even increase. On the other hand, there is no general reason why such intermediate phases with large periodicity cannot be observed at all, and thus they may still be discovered in frustrated smectics of different molecular structure or in mixtures. Therefore, it may be interesting to predict the detailed structure of these intermediate phases theoretically using general arguments without reference to a particular model.

In existing literature the structure of the intermediate phases has been derived using specific theoretical models [17, 19, 20]. In this paper we show that the experimentally observed 3D structure of the intermediate phases can be derived using symmetry arguments in the context of a very general discrete model with practically arbitrary short and long range orientational coupling between different smectic layers. This general model covers all existing models proposed in the literature and includes many other possibilities. The use of the discrete model itself does not lead to any loss of generality in the qualitative sense because the general discrete model corresponds to a limiting case of the general continuum theory with perfect smectic order. After obtaining the structure of the three- and four-layer intermediate phases, which correspond to existing experimental data, we use the same method to derive the general structure of phases with periodicity of five and six layers, which have not yet been observed.

It has been established that scattering of resonant X-ray beams is an efficient method for experimental resolution of the orientational structure of the intermediate smectic phases [9, 10, 24, 25]. Whereas conventional X-ray scattering resolves only the scalar electron density, revealing the positional smectic order, resonant X-ray scattering enables one to study the anisotropy of molecular susceptibility at frequencies close to resonance and, therefore, to study the director distribution in films of smectic liquid crystals. In § 3 we derive expressions describing the resonant X-ray spectra of novel intermediate phases with periods of five and six smectic layers, which can be used to identify them experimentally.

2. General structure of the intermediate phases

In this section we describe the structure of the intermediate phases using the sufficiently general discrete model. In the discrete model, the free energy of a smectic phase is expressed in terms of the pseudovector order parameters $\mathbf{w}_i=(\mathbf{n}_i\times\mathbf{k})(\mathbf{n}_i\cdot\mathbf{k})$ of the individual layers i [26, 27], where $\mathbf{k}$ is the layer normal and $\mathbf{n}_i$ is the director in the layer i. One notes that the free energy of a single layer depends only on the square $w_i^2=\sin^2 2\Theta/4$, where Θ is the tilt angle, i.e. on $\cos\Theta=(\mathbf{n}_i\cdot\mathbf{k})$. At the same time, a coupling between different layers i and j is expressed in terms of a coupling between the vectors $\mathbf{w}_i$ and $\mathbf{w}_j$. In the general case, the non-chiral interlayer interaction potential is a function of the scalar product $(\mathbf{w}_i\cdot\mathbf{w}_j)$, while the chiral interaction potential between layers i and j is generally proportional to the pseudoscalar $((\mathbf{w}_i\times\mathbf{w}_j)\cdot\mathbf{k})$. For example, taking into account only interactions between adjacent layers, the free energy of a smectic phase per unit area of smectic layers can be written in the following simple form [17], with all higher order coupling terms being neglected:

$$F=\sum_j\left[F_0\left(\sin^2 2\Theta\right)-\frac{1}{2}\Delta\left(\mathbf{w}_j\cdot\mathbf{w}_{j+1}\right)-\frac{1}{2}b_{\mathrm{Q}}\left(\mathbf{w}_j\cdot\mathbf{w}_{j+1}\right)^2-\lambda\left(\left(\mathbf{w}_j\times\mathbf{w}_{j+1}\right)\cdot\mathbf{k}\right)\right] \tag{1}$$

where the first term governs the SmA–SmC phase transition within a layer at a certain temperature T_{AC}, $F_0\propto(T-T_{\mathrm{AC}})$, Δ is the linear coupling coefficient between adjacent layers, b_{Q} is the biquadratic one, and λ characterizes chiral interactions. It should be noted that chiral tilted smectic phases possess a spontaneous polarization in every layer in a direction perpendicular to the tilt plane, i.e. $\mathbf{P}_i\sim\mathbf{w}_i$. In this case, the free energy also contains the so-called 'piezoelectric' coupling term [26] $\mu_{\mathrm{p}}(\mathbf{w}_i\cdot\mathbf{P}_i)$, the standard dielectric term $(1/\chi_\perp)P_i^2$ and several terms describing polarization coupling between neighbouring layers [17, 21]. However, after averaging the total free energy over polarization distribution one obtains the effective free energy which is expressed only in terms of the functions $(\mathbf{w}_i\cdot\mathbf{w}_j)$ and $((\mathbf{w}_i\times\mathbf{w}_j)\cdot\mathbf{k})$ for different i and j. In particular, it has been shown [17] that the linear polarization coupling between adjacent layers results in effective long range coupling between order parameters $\mathbf{w}_i$ in different layers.

Now let us define the azimuthal angle ϕ_i which specifies the orientation of the vector $\mathbf{w}_i$ in the layer i. Taking into account that the vectors $\mathbf{w}_i$ are always parallel to the smectic plane one obtains $(\mathbf{w}_i\cdot\mathbf{w}_j)=\cos(\phi_i-\phi_j)$ and $((\mathbf{w}_i\times\mathbf{w}_j)\cdot\mathbf{k})=\sin(\phi_j-\phi_i)$. Therefore, the arbitrary effective coupling between any two layers i and j depends only on the angle $\phi_{ij}=\phi_j-\phi_i$, and thus in the general case the effective free energy of the tilted smectic phase can be written as

$$F=\sum_i F_i(\Theta)+\sum_{i\neq j} f_{|j-i|}\left(\phi_j-\phi_i\right) \tag{2}$$

where $f_{|j-i|}(\phi_j-\phi_i)$ is some function of the angle $\phi_j-\phi_i$, and $F_i(\Theta)$ is the free energy of a single layer. Note that we have made the common assumption of equal tilt angle in all layers, since there exists no evidence of the opposite.

One notes that the general expression (2) covers all existing discrete models for tilted smectic phases including those used in [16–21]. The free energy (2) can be used to describe the general 3D structure of the intermediate phases with different periodicity without referring to a particular model. Below we first consider phases with periodicity of three and four layers, and compare the results to the experimental data. Then we predict the possible structure of the intermediate phases with periods of five and six smectic layers, which have not yet been observed experimentally.

2.1. *Three-layer subphase*

The structure of the intermediate smectic phase with periodicity of three layers is determined by three angles α_1, α_2 and α_3, where $\alpha_i=\phi_{i+1}-\phi_i$, $i=1, 2, 3$, and the numbers 1, 2, 3 are used to enumerate the smectic layers in the unit cell. The angles α_1, α_2 and α_3 satisfy the condition $\alpha_1+\alpha_2+\alpha_3=2\pi$. Now it can be shown that the general free energy (2) can be written as a symmetric function of α_1, α_2 and α_3. Indeed, let us first consider a coupling between some layer which we denote as '1' and all other layers in the infinite system. In the phase with the three-layer unit cell the interaction between layer '1' and the next layer '2' is generally expressed as $f_1(\alpha_1)$. Taking into account also couplings with all other layers which are equivalent to layer 2 (i.e. with all layers $j=2+3l$ which are separated from layer 2 by an integer number l of periods), one obtains the following expression for the corresponding part of the free energy:

$$\Delta F_{12}=\tilde{f}_1^{(3)}(\alpha_1)=\sum_l f_{|1+3l|}(\alpha_1). \tag{3}$$

In a similar way one obtains an expression for the coupling between layer 1 and all layers j such that $\mathbf{w}_j=\mathbf{w}_3$, where $\mathbf{w}_3$ is the tilt order parameter of layer 3 in the unit cell:

$$\Delta F_{13}=\tilde{f}_2^{(3)}(\alpha_1+\alpha_2)=\sum_l f_{|2+3l|}(\alpha_1+\alpha_2). \tag{4}$$

Here we have taken into account that the angle between $\mathbf{w}_1$ and $\mathbf{w}_3$ is equal to $\alpha_1+\alpha_2$.

Now we take into consideration that in the three-layer intermediate smectic phase an arbitrary layer j is characterized by the same orientation of the vector $\mathbf{w}_j$ as one of the layers 1, 2 or 3 in the unit cell. Thus the sum $\Delta F_1=\Delta F_{12}+\Delta F_{13}+const$ presents the total coupling between layer 1 and all other layers in the system. Similar expressions can be obtained for the coupling between layers 2 or 3 in the unit cell and all other layers. As a result, the total free energy of the three-layer intermediate phase can be expressed as:

$$\begin{aligned}3F_3/N=3F(\Theta)+\tilde{f}_1^{(3)}(\alpha_1)+\tilde{f}_1^{(3)}(\alpha_2)+\tilde{f}_1^{(3)}(\alpha_3)\\+\tilde{f}_2^{(3)}(\alpha_1+\alpha_2)+\tilde{f}_2^{(3)}(\alpha_2+\alpha_3)+\tilde{f}_2^{(3)}(\alpha_1+\alpha_3)+\tilde{f}_0^{(3)}(\Theta)\end{aligned} \tag{5}$$

where the function $\tilde{f}_0^{(3)}(\Theta)$ represents the total coupling between all layers i and j with $\mathbf{w}_i=\mathbf{w}_j$.

One notes that the free energy (5) is invariant under the following permutation of angles:

$$\alpha_1\leftrightarrow\alpha_2;\ \alpha_2\leftrightarrow\alpha_3;\ \alpha_1\leftrightarrow\alpha_3.$$

This means that if the three-layer intermediate phase is formed without secondary symmetry breaking (which may lead to violation of the symmetry presented above), two of the angles α_1, α_2, α_3 must be equal. For example, one obtains $\alpha_1=\alpha_2$ and $\alpha_3=2(\pi-\alpha_1)$ taking into account that $\alpha_1+\alpha_2+\alpha_3=2\pi$. It should be noted that the two other solutions, i.e $\alpha_1=\alpha_3$ or $\alpha_2=\alpha_3$, correspond to exactly the same structure, but with a different enumeration of smectic layers. The corresponding structure of the three-layer intermediate phase, which is schematically represented in figure 1, exactly corresponds to the experimental data [11, 12].

Finally one notes that in principle the symmetry of this structure can be further broken leading, for example, to $\alpha_1\neq\alpha_2$. In this case, however, the existence of the two different stable states with the same free energy would lead to the formation of domains. Such domains have not been observed experimentally, at least for the existing subphases. Thus we assume for the rest of this paper that secondary symmetry breaking in the intermediate phases does not occur.

2.2. *Four-layer intermediate phase*

The general structure of the four-layer intermediate smectic phase can be derived using the same method that has been employed for the description of the three-layer phase. The orientational structure of the four-layer phase is characterized by four angles α_i, $i=1, 2, 3,$

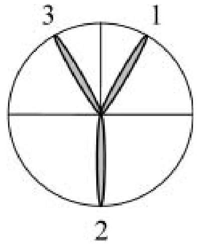

Figure 1. Schematic structure of the three-layer intermediate smectic phase.

4, between the vector order parameters $\mathbf{w}_i$ in neighbouring layers. In such a phase, the orientation of the vector $\mathbf{w}_j$ in an arbitrary layer j is equal to that in one of the four layers $i=1, 2, 3, 4$ within the unit cell. Similar to the three-layer phase, the coupling between layer 1 in some unit cell and all other layers in the system can be expressed as:

$$\Delta F_1 = \tilde{f}_1^{(4)}(\alpha_1) + \tilde{f}_2^{(4)}(\alpha_1+\alpha_2) + \tilde{f}_3^{(4)}(\alpha_1+\alpha_2+\alpha_3) \qquad (6)$$

where

$$\begin{aligned} \tilde{f}_1^{(4)}(\alpha_1) &= \sum_l f_{|1+4l|}(\alpha_1) \\ \tilde{f}_2^{(4)}(\alpha_1+\alpha_2) &= \sum_l f_{|2+4l|}(\alpha_1+\alpha_2) \\ \tilde{f}_3^{(4)}(\alpha_1+\alpha_2+\alpha_3) &= \sum_l f_{|3+4l|}(\alpha_1+\alpha_2+\alpha_3) \end{aligned} \qquad (7)$$

and the first term in equation (6) represents a total coupling between layer 1 and all layers with $\mathbf{w}_j=\mathbf{w}_2$. Here the number 2 corresponds to the second layer in the unit cell, which starts from layer 1. Similarly, the second term represents the coupling between layer 1 and all layers with $\mathbf{w}_j=\mathbf{w}_3$, and the third term represents a coupling with all layers j such that $\mathbf{w}_j=\mathbf{w}_4$ (note that the angle between $\mathbf{w}_1$ and $\mathbf{w}_4$ is equal to $\alpha_1+\alpha_2+\alpha_3$).

Essentially the same expressions also describe the coupling between layers 2, 3 and 4 in the unit cell and all other layers in the system. For example, the coupling of layer 2 with all other layers is given by equations (6, 7), where all angles α_i, $i=1, 2, 3, 4$, are replaced by α_{i+1} with $\alpha_5{:=}\alpha_1$. As a result, the free energy of the four-layer intermediate phase can be written in a form similar to equation (5)

$$\begin{aligned} 4F_4/N = {} & 4F(\Theta) + \tilde{f}_1^{(4)}(\alpha_1) + \tilde{f}_1^{(4)}(\alpha_2) + \tilde{f}_1^{(4)}(\alpha_3) \\ & + \tilde{f}_1^{(4)}(\alpha_4) + \tilde{f}_2^{(4)}(\alpha_1+\alpha_2) + \tilde{f}_2^{(4)}(\alpha_2+\alpha_3) \\ & + \tilde{f}_2^{(4)}(\alpha_3+\alpha_4) + \tilde{f}_2^{(4)}(\alpha_1+\alpha_4) \\ & + \tilde{f}_3^{(4)}(\alpha_2+\alpha_3+\alpha_4) + \tilde{f}_3^{(4)}(\alpha_3+\alpha_4+\alpha_1) \\ & + \tilde{f}_3^{(4)}(\alpha_4+\alpha_2+\alpha_1) + \tilde{f}_0^{(4)}(\Theta) \end{aligned} \qquad (8)$$

where the general formulae for the functions $\tilde{f}_n^{(4)}(\ldots)$, $n=1, 2, 3$ reads

$$\tilde{f}_n^{(4)}\left(\sum_m \alpha_m\right) = \sum_l f_{|n+4l|}\left(\sum_m \alpha_m\right) \qquad (9)$$

and the function $\tilde{f}_0^{(4)}(\Theta)$ describes the coupling between all pairs of layers with the same orientation of the order parameter $\mathbf{w}$.

Similarly to the three-layer phase, the general structure of the four-layer intermediate phase is determined by the symmetry of the free energy. Indeed, the free energy (8) is invariant under the following two sets of angle permutation:

$\alpha_1 \leftrightarrow \alpha_2$ and $\alpha_3 \leftrightarrow \alpha_4$
or
$\alpha_1 \leftrightarrow \alpha_3$ and $\alpha_2 \leftrightarrow \alpha_4$.

One notes that these two sets of permutations correspond to two different structures of the four-layer unit cell. The first structure is characterized by $\alpha_1=\alpha_2$ and $\alpha_3=\alpha_4$, while the second one corresponds to $\alpha_1=\alpha_3$ and $\alpha_2=\alpha_4$. Both structures, which are schematically presented in figure 2, are allowed from the symmetry point of view. One of them, figure 2 (*b*), has indeed been observed by experiment [8, 10]. Finally, one notes that both structures presented in figure 2 correspond to the condition $\alpha_1+\alpha_2+\alpha_3+\alpha_4=2\pi$ and thus $\alpha_1=\pi-\alpha_2$ in figure 2 (*b*). For the four-layer phase the sum of all angles α_i may also be equal to 4π. In this case, however, one obtains the structure which corresponds to the ideal anticlinic antiferroelectric $\mathrm{SmC}_\mathrm{A}^*$ phase which has a two smectic layers period.

2.3. *Two possible structures of the five-layer intermediate phase*

In the five-layer intermediate phase, the orientational structure of the unit cell is characterized by five angles α_i, $i=1$–5, which satisfy the condition $\sum_{i=1}^{5}\alpha_i=2\pi k$ where $k=1$ or 2. Now let us select an arbitrary unit cell in the infinite system of smectic layers, and consider the total coupling between layer 1 in this unit cell and all other layers in the system. Similarly to the case of the four-layer structure the total coupling can be expressed as

$$\begin{aligned} \Delta F_1^{(5)} = {} & \tilde{f}_1^{(5)}(\alpha_1) + \tilde{f}_2^{(5)}(\alpha_1+\alpha_2) + \tilde{f}_3^{(5)}(\alpha_1+\alpha_2+\alpha_3) \\ & + \tilde{f}_4^{(5)}(\alpha_1+\alpha_2+\alpha_3+\alpha_4) \end{aligned} \qquad (10)$$

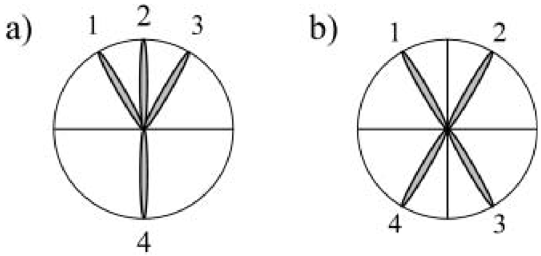

Figure 2. Two possible structures of the four-layer intermediate smectic phase. The structure (*a*) has been observed experimentally. See text for details.

where

$$\tilde{f}_i^{(5)}\left(\sum_{j=1}^{i}\alpha_j\right)=\sum_l f_{|i+4l|}\left(\sum_{j=1}^{i}\alpha_i\right) \tag{11}$$

and $i=1, 2, 3, 4$. Here the function $\tilde{f}_i^{(5)}$ is a sum of all coupling terms between layer 1 and all those layers j which have the same orientation of the vector $\mathbf{w}_j$ as in layer $1+i$ within the unit cell, i.e. $\mathbf{w}_j=\mathbf{w}_{i+1}$.

Now the total coupling between all layers in an arbitrary unit cell and all other layers in the system (including those within the same unit cell) can be expressed as a sum of the expressions similar to equation (10) for all five layers in the unit cell. As a result, the total free energy of the five-layer phase can be written in the form

$$\begin{aligned}5F_5/N=5F(\Theta)&+\sum_{i=1}^{5}\tilde{f}_1^{(5)}(\alpha_i)+\sum_{i=1}^{5}\tilde{f}_2^{(5)}(\alpha_i+\alpha_{i+1})\\&+\sum_{i=1}^{5}\tilde{f}_3^{(5)}(\alpha_i+\alpha_{i+1}+\alpha_{i+2})\\&+\sum_{i=1}^{5}\tilde{f}_4^{(5)}(\alpha_i+\alpha_{i+1}+\alpha_{i+2}+\alpha_{i+3})\end{aligned} \tag{12}$$

where $\alpha_6:=\alpha_1$; $\alpha_7:=\alpha_2$ and $\alpha_8:=\alpha_3$, and the coefficients $\tilde{f}_j^{(5)}$ are given by equation (11).

It can be shown that the free energy (12) is invariant under the transformation: $\alpha_1\leftrightarrow\alpha_5$, $\alpha_2\leftrightarrow\alpha_4$.

Thus there exist two possible structures of the five-layer intermediate phase. Both structures are characterized by $\alpha_1=\alpha_5$ and $\alpha_2=\alpha_4$ but, at the same time, they differ by the value of k. The first structure presented in figure 3 (*a*) corresponds to the total rotation of the tilt within the unit cell equal to 2π, i.e. $k=1$. The second structure, figure 3 (*b*), corresponds to $k=2$. This structure has also been obtained by a direct minimization of the free energy using a particular model [17]. It is interesting to note that the two structures in figure 3 differ qualitatively only by the distribution of layers with a given tilt within the unit cell. One notes also that the cyclic permutation of indices 1, 2, 3, 4, 5 can be applied to all expressions presented in this section. Such permutations only change the enumeration of layers and do not create new structures.

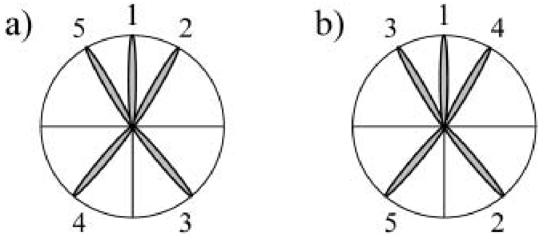

Figure 3. Two possible structures of the five-layer intermediate smectic phase. The structure (*a*) has also been obtained using a particular model [17]. See text for details.

2.4. *Possible structures of the six-layer intermediate phase*

Equation (12) for the free energy of the five-layer phase can readily be generalized to the case of the six-layer phase. Taking into account that the free energy of the six-layer intermediate phase depends on six angles α_i, $i=1$–6, one obtains:

$$\begin{aligned}6F_6/N=6F(\Theta)&+\sum_{i=1}^{6}\tilde{f}_1^{(6)}(\alpha_i)+\sum_{i=1}^{6}\tilde{f}_2^{(6)}(\alpha_i+\alpha_{i+1})\\&+\sum_{i=1}^{6}\tilde{f}_3^{(6)}(\alpha_i+\alpha_{i+1}+\alpha_{i+2})\\&+\sum_{i=1}^{6}\tilde{f}_4^{(6)}(\alpha_i+\alpha_{i+1}+\alpha_{i+2}+\alpha_{i+3})\\&+\sum_{i=1}^{6}\tilde{f}_5^{(6)}(\alpha_i+\alpha_{i+1}+\alpha_{i+2}+\alpha_{i+3}+\alpha_{i+4})\end{aligned} \tag{13}$$

where $\alpha_6:=\alpha_1$; $\alpha_7:=\alpha_2$, $\alpha_8:=\alpha_3$ and $\alpha_9:=\alpha_4$, and the coefficients $\tilde{f}_j^{(5)}$ are given by relationships analogous to equations (11).

Similarly to the previous two sections, it can be shown that the free energy (13) is invariant under the following two sets of transformation of angles: $\alpha_1\leftrightarrow\alpha_4$, $\alpha_2\leftrightarrow\alpha_5$, $\alpha_3\leftrightarrow\alpha_6$; or $\alpha_1\leftrightarrow\alpha_6$, $\alpha_2\leftrightarrow\alpha_5$, $\alpha_3\leftrightarrow\alpha_4$.

Thus, for each value of k there are two possible structures of the six-layer intermediate phase which are characterized by the relationships $\alpha_1=\alpha_4$, $\alpha_2=\alpha_5$, $\alpha_3=\alpha_6$

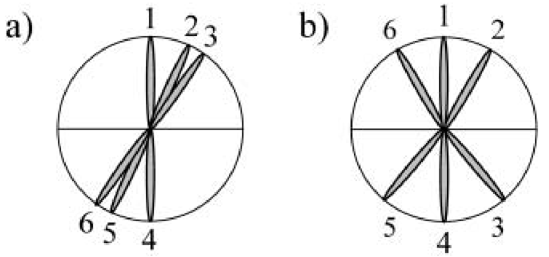

Figure 4. Two possible structures of the predominantly uniaxial six-layer intermediate smectic phase. The structure (*b*) has also been obtained using a particular model [19]. See text for details.

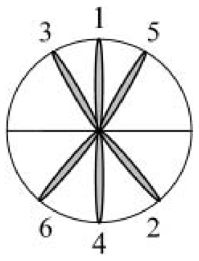

Figure 5. Possible structure of the predominantly inclined six-layer intermediate smectic phase. The tilting directions of the 1st and 4th layers coincide.

or $\alpha_1=\alpha_6$, $\alpha_2=\alpha_5$, $\alpha_3=\alpha_4$. The two structures which correspond to $k=1$ (i.e which correspond to the total rotation of the tilt in the unit cell equal to 2π) are schematically presented in figure 4. Intuitively, the more symmetric structure presented in figure 4 (*b*) seems to be the more favourable one. This structure has been obtained by the minimization of the free energy in another particular model [19]. The only possible structure, which corresponds to $k=2$, is presented in figure 5. Unlike the structures in figure 4, it is considerably asymmetric and the molecules are tilted predominantly in one direction. The similar $k=2$ analogue of the structure from figure 4 (*a*) is absent, since it would possess a three-layer periodicity.

It should be noted that equation (13) can be generalized to the case of arbitrary large period. The corresponding expression, however, is very cumbersome and will not be presented in this paper.

3. Resonant X-ray spectra of intermediate phases with five- and six-layer periodicity

The general theoretical background that enables one to resolve the director distribution within the unit cell of a smectic phase, using the observable intensities of resonant satellite peaks, is well described in [24, 25, 28]. Below we briefly view the main steps of the calculations and consider the special features of resonant X-ray scattering from the structures predicted in the previous section.

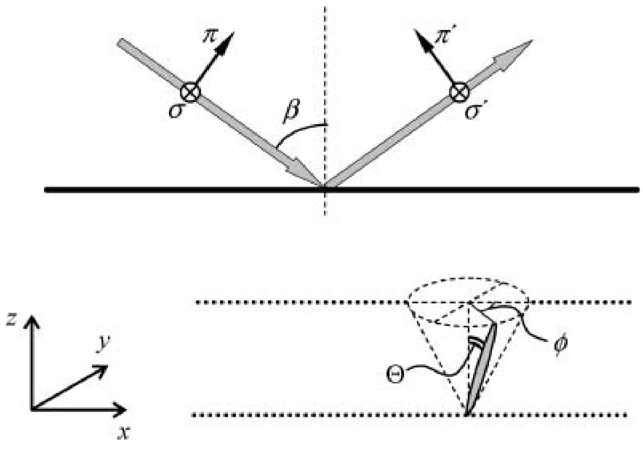

Figure 6. The scheme of the resonant X-ray experiment.

The scheme of the X-ray experiment is presented in figure 6. In contrast to conventional X-ray methods, in this case one should take into account the polarization degree of freedom and therefore consider the tensorial susceptibility of the medium. One notes that the single smectic layer susceptibility tensor has a diagonal form in the coordinate system tilted together with the director:

$$\hat{\chi}_{\mathrm{s}}(z)=\begin{pmatrix}\chi_0(z) & 0 & 0\\ 0 & \chi_0(z) & 0\\ 0 & 0 & \chi_0(z)+\chi_{\mathrm{A}}(z)\end{pmatrix}. \qquad (14)$$

Here the z-dependent susceptibility components are expected to decay at smectic layer thickness L. Since the anisotropic resonant part usually arises due to specific atomic inclusions in the molecules, $\chi_{\mathrm{A}}(z)$ should be localized at a smaller length scale.

The total susceptibility can easily be expressed using the rotation matrices $\hat{R}^{(i)}_{\phi}$ which describe the rotation by an angle ϕ around the i-axis:

$$\hat{\chi}(z)=\sum_{t=-\infty}^{\infty}\sum_{n=1}^{N}\hat{R}^{(z)}_{\phi_n}\hat{R}^{(y)}_{\Theta}\hat{\chi}_{\mathrm{s}}(z+NtL+nL)\hat{R}^{(y)}_{-\Theta}\hat{R}^{(z)}_{-\phi_n}. \qquad (15)$$

Here the summation is undertaken first over layers n through the N-layered unit cell and then over all the unit cells. Again, the structure of the unit cell and its orientation as a whole is specified by the set of N angles $\{\phi_n\}$, which are measured from the x-axis as shown in figure 6.

Combining equations (14) and (15) and performing the Fourier transformation with respect to the z-dependence one finally obtains the susceptibility as a function of the wave vector q parallel to the z-axis, which can be transferred to the medium during scattering. The resonant anisotropy leads to a small tensorial contribution to the scalar conventional peaks, which possess the wave vectors equal to multiples of $2\pi/L$. In addition, $(N-1)$ equidistant satellites occur generally between the conventional peaks. The corresponding part of the susceptibility reads

$$\hat{\chi}_{\mathrm{anis}}(q)=\frac{\pi}{L}\chi_{\mathrm{A}}(q)\sum_{s=-\infty}^{\infty}\delta\left(q-\frac{2\pi s}{NL}\right)\sum_{n=1}^{N}\exp\left(-\frac{2\pi i}{N}sn\right)\hat{T}(\Theta,\phi_n) \qquad (16)$$

where we have introduced the tensorial function

$$\hat{T}(\Theta,\phi)=\sin 2\Theta\begin{pmatrix}0 & 0 & \cos\phi\\ 0 & 0 & -\sin\phi\\ \cos\phi & -\sin\phi & 0\end{pmatrix}+\sin^2\Theta\begin{pmatrix}\cos 2\phi & -\sin 2\phi & 0\\ -\sin 2\phi & -\cos 2\phi & 0\\ 0 & 0 & 0\end{pmatrix}. \qquad (17)$$

This function is composed of two terms with completely different tensorial structures. According to established terminology, corresponding satellite peaks are referred to as 1st and 2nd type peaks, respectively. Experimentally the type of the peak can easily be identified by polarization analysis. On the other hand, very often both types contribute to the same peak, giving rise to a hybrid scattering.

For a given polarization of incident and scattered waves, $|i>$ and $|f>$, the scattered wave intensity is proportional to the square of the product $|\langle f|\hat{\chi}|i\rangle|$. The dependence of the satellite intensity on the unit cell structure and experiment geometry is given by the following factors

$$S_s^{(fi)}=\left|\sum_{n=1}^{N}\exp\left(-\frac{2\pi i}{N}sn\right)\langle i|\hat{T}(\Theta,\phi_n)|f\rangle\right|^2. \qquad (18)$$

Here the index $s=1, \ldots, N-1$ denotes the satellite number. Higher s values, which are present in equation (16), correspond to satellites with the same factors (18). Their intensities differ only due to a smooth dependence of χ_A on wave vector in equation (16).

In the analysis of the polarization features we restrict ourselves to the simplest case of σ or π polarized incident and scattered beams (see figure 6). Since the angle of reflection is equal to the angle of incidence, β, we have $<\pi|=(\cos\beta,\ 0,\ \sin\beta)$, $<\pi'|=(-\cos\beta,\ 0,\ \sin\beta)$ and $<\sigma|=<\sigma'|=(0,\ 1,\ 0)$.

Accordingly, the S-factors take the form:

$$S_s^{(\pi'\pi)}=\sin^4\Theta\cos^4\beta|u_1^s|^2,\ S_s^{(\sigma'\sigma)}=\sin^4\Theta|u_1^s|^2 \qquad (19)$$

$$S_s^{(\pi'\sigma)}=\left|\sin 2\Theta\sin\beta\, u_2^s-\sin^2\Theta\cos\beta\, u_3^s\right|^2 \qquad (20)$$

$$S_s^{(\sigma'\pi)}=\left|\sin 2\Theta\sin\beta\, u_2^s+\sin^2\Theta\cos\beta\, u_3^s\right|^2 \qquad (21)$$

where the parameters

$$u_1^s=\sum_{n=1}^{N}\exp\left(-\frac{2\pi i}{N}sn\right)\cos 2\phi_n \qquad (22)$$

$$u_2^s=\sum_{n=1}^{N}\exp\left(-\frac{2\pi i}{N}sn\right)\sin\phi_n \qquad (23)$$

$$u_3^s=\sum_{n=1}^{N}\exp\left(-\frac{2\pi i}{N}sn\right)\sin 2\phi_n \qquad (24)$$

are fully determined by the structure and orientation of the unit cell.

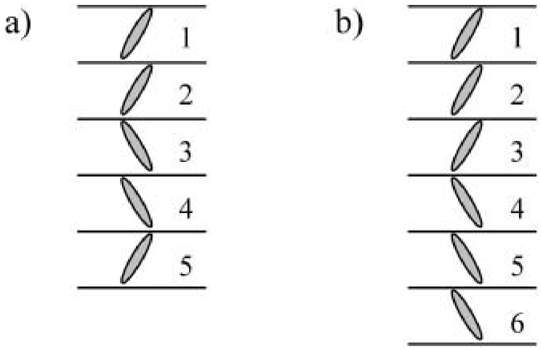

Figure 7. Schematic structures of (*a*) flat five-layer corresponding to figure 3 (*a*), and (*b*) six-layer corresponding to figure 4 (*a*) intermediate smectic phases.

To illustrate this general formulae we turn now to X-ray spectra for two particular structures predicted in the previous section and shown in figures 3 (*a*) and 4 (*a*). Note that according to available experimental data the structure of the three-layer intermediate phase is rather close to flat, i.e., the deviations of angles α_n from 0 or π values are not large. In most cases, the same is also true for the four-layer phase, although a considerably non-flat structure of such a phase has been also reported recently [14]. For the sake of simplicity, we assume here that all the structures of commensurate sub-phases are close to flat. Correspondingly, we start with analysing the X-ray scattering in the case of flat structures (see figure 7) and then describe special features arising from the deviations from flatness.

It is easy to conclude from equation (22) that for a completely flat unit cell rotated by an angle ϕ_0 with respect to the x-axis ($\phi_n=\phi_0$ or $\phi_n=\phi_0+\pi$), the parameters $u_{1,3}^s=0$. Consequently, the state of the X-ray polarization totally flips during scattering, and thus the intensities of $\pi\sigma$ and $\sigma\pi$ scattering are equal. For the five-layered flat structure shown in figure 7 (*a*), the flat prototype of that depicted in figure 3 (*a*), we have $\phi_{1,2,5}=\phi_0$ and $\phi_{3,4}=\phi_0+\pi$, which yields

$$S_s^{(\sigma'\pi)}=S_s^{(\pi'\sigma)}=16\sin^2 2\Theta\sin^2\beta\sin^2\phi_0\cos^2\frac{\pi s}{5}. \qquad (25)$$

The flat six-layered structure seen in figure 7 (*b*) is the flat variant of that in figure 4 (*a*), and there $\phi_{1,2,3}=\phi_0$

and $\phi_{4,5,6}=\phi_0+\pi$. Accordingly, the satellites with even s vanish completely, and

$$S_s^{(\sigma'\pi)} = S_s^{(\pi'\sigma)} = 4\sin^2 2\Theta \sin^2\beta \sin^2\phi_0 \sin^{-2}\frac{\pi s}{6}, \quad s=1,\,3,\,5. \tag{26}$$

It should be noted that in the case of weak deviation from flat structures both $\pi\pi$ and $\sigma\sigma$ scattering appear to be possible. For the five-layer intermediate phase with orientational structure specified by the angles $\phi_1=\phi_0$, $\phi_2=\phi_0+\delta_1$, $\phi_3=\phi_0+\pi-\delta_2$, $\phi_4=\phi_0+\pi+\delta_2$, $\phi_5=\phi_0-\delta_1$, see figure 3 (*a*), with relatively small $\delta_{1,2}$, one obtains:

$$\begin{aligned} S_s^{(\pi'\pi)} &= \cos^4\beta\, S_s^{(\sigma'\sigma)} \\ &= 16\sin^4\Theta \cos^4\beta \sin^2 2\phi_0 \\ &\quad \left[\delta_1 \sin\frac{3\pi s}{5} - \delta_2 \sin\frac{\pi s}{5}\right]^2. \end{aligned} \tag{27}$$

For the six-layered phase with orientational structure specified by $\phi_1=\phi_0$, $\phi_2=\phi_0+\delta_1$, $\phi_3=\phi_0+\delta_2$, $\phi_4=\phi_0+\pi$, $\phi_5=\phi_0+\pi+\delta_1$, $\phi_6=\phi_0+\pi+\delta_2$, see figure 4 (*a*), both $\pi\pi$ and $\sigma\sigma$ satellites appear with $s=2$, 4:

$$\begin{aligned} S_{2,4}^{(\pi'\pi)} &= \cos^4\beta\, S_{2,4}^{(\sigma'\sigma)} \\ &= 4\sin^4\Theta \cos^4\beta \sin^2 2\phi_0 \left(\delta_1^2 - \delta_1\delta_2 + \delta_2^2\right). \end{aligned} \tag{28}$$

Any deviations from the flat structure give rise to a correction to the $\pi\sigma$ and $\sigma\pi$ scattering intensities, equations (25) and (26). However, for the majority of the satellites, the corresponding contribution is extremely small due to the weakness of the deviation. The only exclusions are the $s=2$, 4 satellites in the six-layered intermediate phase, which are absent if the unit cell is completely flat:

$$\begin{aligned} S_{2,4}^{(\sigma'\pi)} &= S_{2,4}^{(\pi'\sigma)} \\ &= 16\sin^4\Theta \cos^2\beta \cos^2 2\phi_0 \left(\delta_1^2 + \delta_1\delta_2 + \delta_2^2\right). \end{aligned} \tag{29}$$

The intensity of these satellites is proportional to a higher power of the tilt angle Θ and thus these peaks are even weaker than the peaks of equations (27) and (28).

In a real X-ray experiment the orientation of the director in a given smectic layer is not necessarily homogeneous within the whole area illuminated by the beam. Domains and/or long range in-plane fluctuations of the tilting direction may lead to a strong spatial variation of the angle ϕ_0 in the plane of the layer. However, all expressions obtained in this section can readily be modified to take the ϕ_0-uncertainty into account by a simple replacement of all squares of trigonometric functions of ϕ_0 in equations (25–29) by the average value of 1/2.

In summary, it has been shown in this section that the spectra of resonant X-ray scattering from five- and six-layered intermediate phases can be used for clear identification of these phases. For example, the existence of the $s=1$, 3, 5 satellites in the six-layered phase enables one to distinguish it from the three-layered phase. In addition, polarization analysis enables us to resolve the unit cell structure of these phases. Indeed, comparing the intensities of the $\pi\sigma$ and $\sigma\pi$ scattering, equations (25) and (26), for different satellites (different s) the structure of the prototype flat phase can be resolved. At the second stage the analysis of weaker $\pi\pi$ an $\sigma\sigma$ scattering enables one to determine the amplitudes of weak deviations from the flat structure.

4. Discussion

It has been shown in this paper that all qualitative features of the actual structure of the intermediate smectic phases can be obtained using the symmetry transformation properties of the general expression for the free energy of the corresponding phases, without addressing a particular model. The general free energy of a smectic phase used in this paper is not based on any particular interlayer interactions but includes practically arbitrary short as well as long range coupling between different smectic layers. We have shown that a unique structure of the three-layer intermediate phase exists (see figure 1) which corresponds to the symmetry of the general free energy. This structure also corresponds to the existing experimental data. In the case of the four-layer phase, two different structures are consistent with the transformation properties of the general free energy (see figure 2). One of these structures has indeed been observed experimentally. Using the same method we have also predicted the possible structures of the five- and six-layer intermediate phases which are presented in figures 3–5. There exist only two qualitatively different structures of the five-layer phase which are consistent with the symmetry of the general free energy. One of these structures also corresponds to the structure obtained after a direct minimization of the free energy in the context of a particular model [17]. Note that the other structure, which corresponds to a total rotation of 4π within the unit cell, contains more 'anticlinic' pairs, while the structure presented in figure 3 (*a*) contains more synclinic pairs. In general, there exist three possible structures of the six-layer intermediate phase which are consistent with the symmetry of the general free energy. One of them, see figure 4 (*b*), has also been obtained using a different model [19]. The structures presented in figures 4 (*b*) and 5 differ qualitatively only by the relative amount of synclinic and anticlinic pairs in the unit cell.

The structures in figures 3–5 are presented here to illustrate qualitatively possible director distributions within a unit cell. The numerical values of the angles between tilt directions in adjacent layers are expected to be different for different materials. At the same time there are several interesting particular cases of the general structures. For example, flat unit cells presented in figure 7 are also consistent with the symmetry of the general free energy. It can be shown, however, that all two-dimensional structures are unstable with respect to any chiral orientational interactions between different smectic layers. One also notes that 'clock' helical structures, in which all angles between tilt directions in adjacent layers are the same, possess higher symmetry than those presented in figures 3 and 4. Also, this higher symmetry does not contradict the transformation properties of the general free energy. The commensurate 'clock' structures, however, have not been observed so far.

In the last section we also obtained explicit analytical expressions which describe resonant X-ray spectra of five- and six-layer intermediate phases with the predicted structure. These spectra are characterized by a number of additional satellites which can readily be identified to distinguish the corresponding intermediate phases from those with smaller periods. In particular, the resonant spectra of the five-layer subphase are characterized by satellites with all possible values of $s=1$, 2, 3, 4. In the case of the six-layer subphase the existence of the $s=1$, 3, 5 satellites enables one to distinguish it from the three-layer subphase. As with the three- and four-layer subphases, in the case of 3D five- and six-layer phases both $\pi\pi$ and $\sigma\sigma$ scattering is also possible for the same value of s. In addition, the six-layer structure is characterized by specific $\pi\pi$ and $\sigma\sigma$ satellites with $s=2$, 4 which are absent in the corresponding six-layer flat structure. These additional peaks are expected to be relatively weak in the case of small tilt angles because their intensity is proportional to $\sin^4 \Theta$.

Finally, it should be noted that we did not consider intermediate phases with periods larger then six layers because it is rather unlikely that such phases can be observed in real systems. Intermediate phases with large periodicity may be suppressed by a number of factors including surface and finite size effects.

Acknowledgments

M.A.O is grateful to H.Gleeson and members of her group for interesting discussions. This work has been supported by the Leverhulme Trust (Research Fellowship RF/4/RFG/2004/0493) and INTAS (project 01-0822).

References

[1] J.W. Goodby (Ed.). *Ferroelectric Liquid Crystals*. Gordon and Breach, New York (1992).

[2] S. Lagerwall. *Ferroelectric and Antiferroelectric Liquid Crystals*. Wiley-VCH, Weinheim (1999).

[3] A. Fukuda, Y. Takanishi, T. Isozaki, K. Ishikawa, H. Takezoe. *J. mater. Chem.*, **4**, 997 (1994).

[4] A.D.L. Chandani, Y. Ouchi, H. Takezoe, A. Fukuda, K. Terashima, K. Furukawa, A. Kishi. *Jpn. J. appl. Phys.*, **28**, L1261 (1989).

[5] T. Fujikawa, H. Orihara, Y. Ishibashi, Y. Yamada, N. Yamamoto, K. Mori, K. Nakamura, Y. Suzuki, T. Hagiwara, I. Kawamura. *Jpn. J. appl. Phys.*, **30**, 2826 (1991).

[6] I. Nishiyama, J.W. Goodby. *J. mater. Chem.*, **2**, 1015 (1992).

[7] P. Mach, R. Pindak, A.-M. Levelut, P. Barois, H.T. Nguyen, C.C. Huang, L. Furenlid. *Phys. Rev. Lett.*, **81**, 1015 (1998).

[8] A. Cady, J.A. Pitney, R. Pindak, L.S. Matkin, S.J. Watson, H.F. Gleeson, P. Cluzeau, P. Barois, A.-M. Levelut, W. Caliebe, J.W. Goodby, M. Hird, C.C. Huang. *Phys. Rev. E*, **64**, 050702R (2001).

[9] P. Mach, R. Pindak, A.-M. Levelut, P. Barois, H.T. Nguyen, H. Baltes, M. Hird, K. Toyne, A. Seed, J.W. Goodby, C.C. Huang, L. Furenlid. *Phys. Rev. E*, **60**, 6793 (1999).

[10] A. Cady, J.A. Pitney, R. Pindak, L.S. Matkin, S.J. Watson, H.F. Gleeson, P. Cluzeau, P. Barois, A.-M. Levelut, W. Caliebe, J.W. Goodby, M. Hird, C.C. Huang. *Phys. Rev. E*, **B 64**, 050702 (2001).

[11] P.M. Johnson, D.A. Olson, S. Pankratz, T. Nguyen, J. Goodby, M. Hird, C.C. Huang. *Phys. Rev. Lett.*, **84**, 4870 (2000).

[12] D.A. Olson, X.F. Fan, P.M. Johnston, A. Cady, C.C. Huang. *Liq. Cryst.*, **29**, 1521 (2002).

[13] S. Jaradat, N. Roberts, Y. Wang, L. Hirst, H.F. Gleeson. *J. mater. Chem.* (2006).

[14] N.W. Roberts, S. Jaradat, L.S. Hirst, et al. *Europhys. Lett.*, **72**, 976 (2005).

[15] J.P.F. Lagerwall, F. Giesselmann, C. Selbman, S. Rauch, G. Heppke, *J. Chem. Phys.* (in the press).

[16] M. Cepic, E. Gorecka, D. Pociecha, B. Zeks, H.T. Nguyen. *J. Chem. Phys.*, **117**, 1817 (2002).

[17] A.V. Emelyanneko, M.A. Osipov. *Phys. Rev. E*, **68**, 051703 (2003).

[18] D.A. Olson, X.F. Fan, A. Cady, C.C. Huang. *Phys. Rev. E*, **66**, 021702 (2002).

[19] P.V. Dolganov, V.M. Zhilin, V.K. Dolganov, E.I. Kats. *Phys. Rev. E*, **67**, 041716 (2003).

[20] B.N. Hamanesh, P.L. Taylor. *Phys. Rev. Lett.*, **93**, 167801 (2004).

[21] M. Cepic, B. Zeks. *Phys. Rev. Lett.*, **87**, 085501 (2001).

[22] A.V. Emelyanenko, M.A. Osipov. *Ferroelectrics*, **309**, 13 (2004).

[23] R. Bruinsma, J. Prost. *J. Phys. (Fr.) II*, **4**, 1209 (1994).

[24] A.-M. Levelut, B. Pansu. *Phys. Rev. E*, **60**, 6803 (1999).

[25] M.V. Gorkunov, S.A. Pikin. *JETP Lett.*, **69**, 243 (1999).

[26] S.A. Pikin, M.A. Osipov. In *Ferroelectric Liquid Crystals*, G. Goodby (Ed.), Gordon and Breach, New York (1992).

[27] M.A. Osipov, S.A. Pikin. *J. Phys. (Fr.) II*, **5**, 1223 (1995).

[28] V.E. Dmitrienko. *Acta Crystallogr. A*, **39**, 29 (1983).